Experimental Characteristics and Performance Analysis of Monolithic InP-Based HEMT Mixers at W-Band

Youngwoo Kwon, *Student Member, IEEE,* Dimitris Pavlidis, *Senior Member, IEEE,* Phil Marsh, Geok-Ing Ng, *Member, IEEE,* and Timothy L. Brock

Abstract— **Experimental characteristics of monolithic InAlAs/InGaAs HEMT mixers are presented together with a theoretical analysis. Experiments at W-band show a maximum conversion gain of 0.9 dB with 2 dBm of LO power level. This is the first demonstration of a monolithic HEMT mixer with conversion gain at W-band. The conversion gain dependence on LO power, RF frequency and gate bias is measured and compared with the theoretical predictions. Good agreement between the theory and experiment could be found.**

I. Introduction

HIGH FREQUENCY receiver functions such as mixing and amplification are very important for space-based sensors, as well as for military and commercial applications. Passive mixers using two-terminal devices such as Schottky diodes have so far been used in most high-frequency receiver circuits. The active FET mixer is another alternative which has been exploited more recently for millimeter-wave applications.

FET mixers have the possibility of providing conversion gain and reasonably low noise figures with lower local oscillator (LO) power requirements than diode mixers. They are particularly attractive for monolithic integrated receiver circuits due to their compatibility with the FET's used for amplifiers and local oscillators. Among the various FET options, HEMT's are the best choice for low power and high frequency applications due to their superior high frequency characteristics, high transconductance and large nonlinearities. Hybrid mixers using conventional AlGaAs/GaAs HEMT's have been demonstrated at 45 and 94 GHz with reasonable conversion loss characteristics [1], [2].

Another alternative for HEMT realization is an InAlAs/InGaAs heterostructure. Discrete HEMT's fabricated on this material have shown state-of-the-art performance, including a maximum oscillation frequency ($f_{\max}$) of 455 GHz [3]. Furthermore, strained designs with excess indium in the channel exhibit better carrier confinement and improved microwave characteristics [4]. Monolithic integrated circuits using this material have started emerging recently, including X-band amplifiers [5], W-band low-noise amplifiers [6], W-band oscillators [7] and a 90 to 180 GHz doubler [8]. A monolithic mixer using strained InAlAs/InGaAs HEMT's has been realized by the authors: this mixer demonstrated 13.5 dB conversion loss at an LO power of -6 dBm [9]. A hybrid mixer using InP-based HEMT's exhibiting conversion gain at 94 GHz has also been presented recently [10].

This paper presents improved experimental results of the monolithic InAlAs/InGaAs HEMT mixer reported by the authors [9]. Technology optimization led to gate length reduction from 0.2 μm to 0.1 μm and the incorporation of a mushroom gate approach in the process employed for the mixers reported in this paper. Higher f_T (150 GHz versus 120 GHz) and $f_{\max}$ (180 GHz versus 120 GHz) could in this way be obtained. Furthermore, the HEMT was pumped with a higher LO power compared with the previous work [9] so that the mixer could be operated at its optimum LO power. These technology and testing improvements allowed the circuit to demonstrate a conversion gain of 0.9 dB at 94 GHz. This is the first demonstration of a monolithic HEMT mixer showing conversion gain at 94 GHz.

Section II describes nonlinear HEMT modeling and the large-signal analysis of HEMT mixers. A simplified mixer analysis method based on harmonic component studies is discussed in Section III. Considerations of a high-frequency figure of merit regarding the conversion gain characteristics of the mixer are also presented. Finally, the experimental performance at W-band is compared with the results of a two-tone harmonic balance analysis in Section IV.

II. Large-Signal Analysis of HEMT Mixers

A large-signal analysis was used to analyze the conversion gain characteristics of HEMT mixers. If the RF power is much lower than the LO pumping signal, then the large-signal transistor characteristics can be assumed to be unaffected by the presence of the RF signal. The large-signal mixer analysis problem can, in this case, be simplified to a large-signal single-tone consideration (LO) combined with a small-signal analysis (RF). The large-signal characteristics of equivalent circuit parameters are first calculated under single-tone LO excitation. Next, the Fourier components of the equivalent-circuit parameters are used as input parameters of a linear analysis under small-signal RF excitation. Conversion gain

Manuscript received Aug. 22, 1991; revised Apr. 13, 1992. This work was supported by NASA under contract NAGW-1334 and URI under contract DAAL 03-87-K-0007.

The authors are with the Center for Space Terahertz Technology, Solid State Electronics Laboratory, Department of Electrical Engineering and Computer Science, The University of Michigan, Ann Arbor, MI 48109-2122.

IEEE Log Number 9204043.

0018–9480/93$03.00

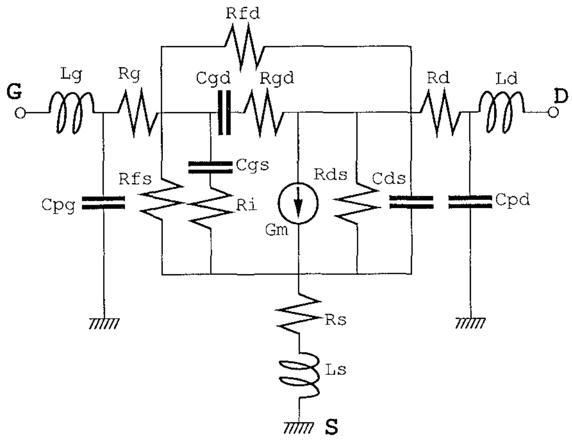

Fig. 1. Small-signal equivalent circuit of HEMT.

characteristics are dependent in this way on the harmonic contents of nonlinear equivalent circuit parameters.

This large-signal single-tone analysis approach was used in this work by carefully accounting for the nonlinear behavior of the HEMT's. A quasi-static large-signal HEMT model based on the bias dependent small-signal S-parameters was developed. A harmonic-balance program was then used to determine the waveform of local oscillator signal at the transistor under the single-tone excitation. Following this, the harmonic components of the time-varying equivalent circuit parameters were found, along with their effects on the mixer performance. This permitted the physical understanding of the mixing and conversion gain saturation mechanisms. Additionally, a two-tone harmonic balance analysis, which included an accurate model for passive elements to account for mismatches and losses coming from them, was performed in order to predict the conversion gain.

The key to the successful large-signal analysis of the circuit is an accurate nonlinear device modeling. The HEMT model used in the analysis is based on the FET model shown in Fig. 1. The small-signal S-parameters were measured over a broad range of bias points. This ensured that the analysis of the mixer could be performed over its entire range of operation. A parameter extraction program following the direct extraction technique of Berroth and Bosch's [11] was developed with some modifications in extracting the parasitic elements. This program uses the minimum number of optimization loops and is thus very efficient for fitting multi-bias S-parameters. A two-dimensional cubic spline interpolation was then employed to describe the bias dependence of the nonlinear equivalent circuit parameters.

In our experience, the use of existing bias-dependence formulae derived for MESFET's gives poor fits for InP-based HEMT's due to their highly nonlinear characteristics: i.e., HEMT's have transconductance characteristics distinctly different from MESFET's. The HEMT transconductance presents a sharp peak at a certain gate-source voltage (V_{gs}) and decreases at high V_{gs} values due to a parasitic channel formation in the low-mobility barrier region. Depending on the doping level of the barrier layer and recess depth, this action may in fact take place before the gate voltage becomes high enough to turn on the Schottky-gate junction.

The interpolation techniques used in this work do not utilize predefined bias dependence formulae and thus provide better flexibility in describing the nonlinear element characteristics; therefore, they are very suitable for modeling highly nonlinear devices such as InAlAs/InGaAs HEMT's. Furthermore, the cubic spline function used in this work gives higher accuracy in terms of interpolation errors compared with polynomial or square root fitting. Accurate reproduction of experimental microwave data over the voltage range of interest was thus possible even with a limited number of measured data.

In this work, the following six elements were assumed to be nonlinear: (i) transconductance (g_m), (ii) drain-source resistance (r_{ds}), (iii) gate-source capacitance (c_{gs}), (iv) gate-drain capacitance (c_{gd}), (v) gate-source resistance (r_{fs}), (vi) gate-drain resistance (r_{fd}). The results obtained for the HEMT's of this study indicate that it is reasonable to assume that the other parameters are voltage-independent linear elements.

Monolithic HEMT mixers using two different device characteristics were fabricated and tested. The high frequency properties of the mixers were investigated and the effect of transconductances on their performance was studied. The spline interpolation representations of the transconductances of the two HEMT's are shown in Fig. 2 as constructed from a matrix of $7V_{gs}$ and $6V_{ds}$ points. HEMT A shows higher peak transconductance and more rapid variation with V_{gs}. The details of the device characteristics will be addressed in Sections III and IV.

III. Harmonic Content of HEMT Parameters

The harmonic content studies were performed as outlined in Section II by exciting the device with a single-tone variable-power LO. The nonlinear transistor parameters (denoted as $x(t)$ and representing g_m, r_{ds}, c_{gs} and c_{gd}) vary periodically with the LO waveform and can be described with the help of Fourier coefficients X_k's with a fundamental frequency equal to the LO signal frequency (ω_{LO}):

$$x(t) = \sum_{k=-\infty}^{\infty} X_k e^{jk\omega_{\mathrm{LO}} t}. \tag{1}$$

The capacitance and conductance waveform can be found from the single-tone harmonic balance analysis and their harmonic contents (X_k's) can be calculated using a fast Fourier transformation.

Among the four major nonlinear elements considered in this work, the nonlinearities of g_m and r_{ds} are more significant than those of c_{gs} and c_{gd}. This is true provided that the drain bias remains in the saturation region and the LO power level is not so high as to turn the Schottky gate on; gate leakage becomes in this case important and degrades the transistor performance. The c_{gs} and c_{gd} nonlinearities were consequently neglected in the first-order calculation reported in this section. They were, however, considered in the full two-tone harmonic balance simulations described in Section IV, c_{gs} is in fact playing a major role in degrading the conversion gain achievable with a HEMT when the device is operated at very high

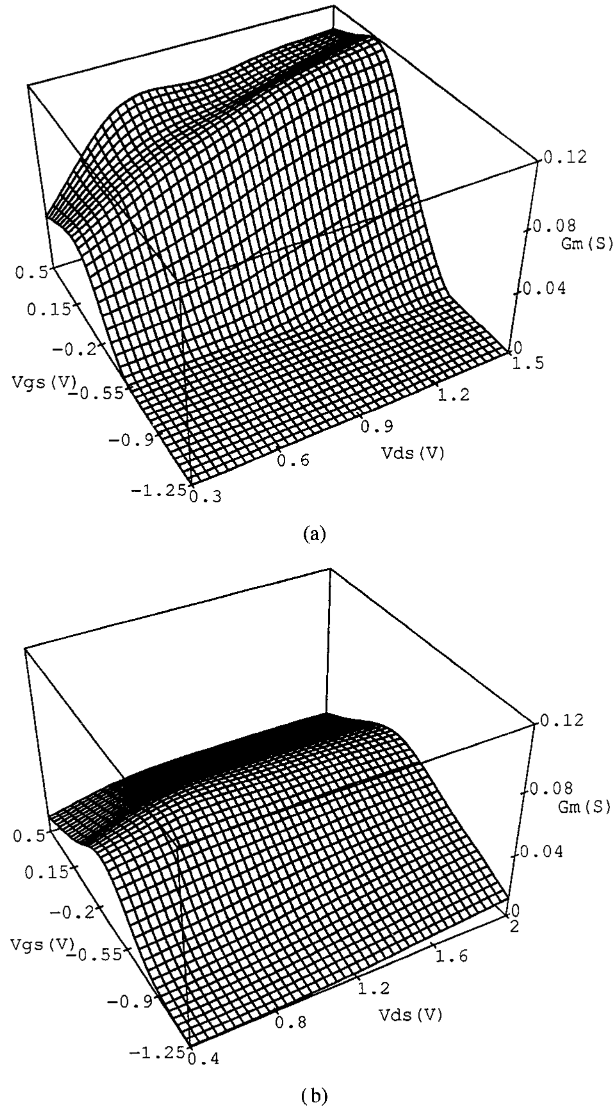

Fig. 2. Spline interpolation representation of HEMT transconductance: (a) HEMT A. (b) HEMT B.

frequencies where displacement current effects become very important.

Between the two strongest nonlinearities, namely g_m and r_{ds}, the latter does not play an important role in the mixing mechanism because of the low load termination at the IF port. This arises from the following considerations. IF conjugate matching is usually hard to achieve in mixer designs since it may result in transistor instability. Consequently, an impedance value lower than the output resistance is often used to terminate the drain port. The mixing effect of the output resistance is thus reduced by paralleling it with a small load resistance and can be ignored for qualitative mixing mechanism studies. This is especially true when the transconductance nonlinearity is much more significant than any other nonlinearities as is the case with the InP-based HEMT's of this work.

Thus, it is reasonable to consider the transconductance as the only time-varying element and give qualitative explanations concerning the conversion gain characteristics of HEMT mixers. This approach may not provide an exact estimation of conversion gain. However, the physical understanding of mixing mechanism and a simple high-frequency figure of merit can be obtained in this way.

The harmonic components of the transconductance waveform are compared in Fig. 3 for HEMT's A and B for various LO pumping power levels. Following Pucel *et al.* [12], when the gate is conjugately matched while the drain is matched for the imaginary part only, the conversion gain (G_c) is related to the first harmonic component of g_m (g_{m_1}) as follows.

$$G_c = \frac{g_{m_1}^2}{\omega_{\mathrm{RF}}^2 \overline{c}_{gs}^2} \cdot \frac{R_{\mathrm{load}}}{R_{\mathrm{in}}} \cdot \frac{1}{\left(1 + \frac{R_{\mathrm{load}}}{\overline{r}_{ds}}\right)^2}. \tag{2}$$

The above expression assumes that the IF frequency is much lower than the RF frequency and the first harmonic of g_m is the only nonlinear component. The estimated time averages are used for the parameters $\overline{c}_{gs}$ and $\overline{r}_{ds}$. These were obtained from the dc components of Fourier representation of $c_{gs}(t)$ and $r_{ds}(t)$. R_{in} is the real part of the input impedance and R_{load} is the real part of the IF load. From (2), it is obvious that the conversion gain of the FET mixer is determined by the first harmonic component of transconductance (g_{m_1}).

Fig. 3 shows that the first harmonic component of the transconductance (g_{m_1}) increases with LO pumping power up to a certain power level and degrades at high LO drive for both HEMT's. This can be understood by considering the gate bias dependence of transconductance given in Fig. 2. As the instantaneous gate voltage passes the maximum g_m point, both the value of g_m and its first harmonic component decrease.

The HEMT mixer conversion gain shows similar LO power dependence as the transconductance. In fact, the particular transconductance features determine the major difference between HEMT and MESFET mixers with respect to their LO power dependence. Compared with MESFET's, HEMT's generally have sharper $g_m - V_{gs}$ characteristics and higher transconductance values. Higher conversion gain should therefore be possible using lower LO power in HEMT's. Among the two tested HEMT's, HEMT A has a larger peak g_{m_1} value than HEMT B, and the peak value occurs at a lower $V_{gs} - V_p$ (V_p: pinch-off voltage) or equivalently lower LO power level. This implies that the optimum LO power drive is expected to be lower in a mixer using HEMT A.

The magnitude of conversion gain is not, however, solely dependent on g_{m_1}, but on the ratio of $g_{m_1}/\overline{c}_{gs}$ as shown by (2). Based on this observation, one can define an intrinsic cutoff frequency concerning the first harmonic component of the transconductance $(f_{T,g_{m_1}})$ as follows:

$$f_{T,g_{m_1}} \equiv \frac{g_{m_1}}{2\pi \overline{c}_{gs}} \tag{3}$$

Equation (2) can then be rewritten in the following form:

$$G_c = \left(\frac{f_{T,g_{m_1}}}{f_{\mathrm{RF}}}\right)^2 \cdot \frac{R_{\mathrm{load}}}{R_{\mathrm{in}}} \cdot \frac{1}{\left(1 + \frac{R_{\mathrm{load}}}{\overline{r}_{ds}}\right)^2}. \tag{4}$$

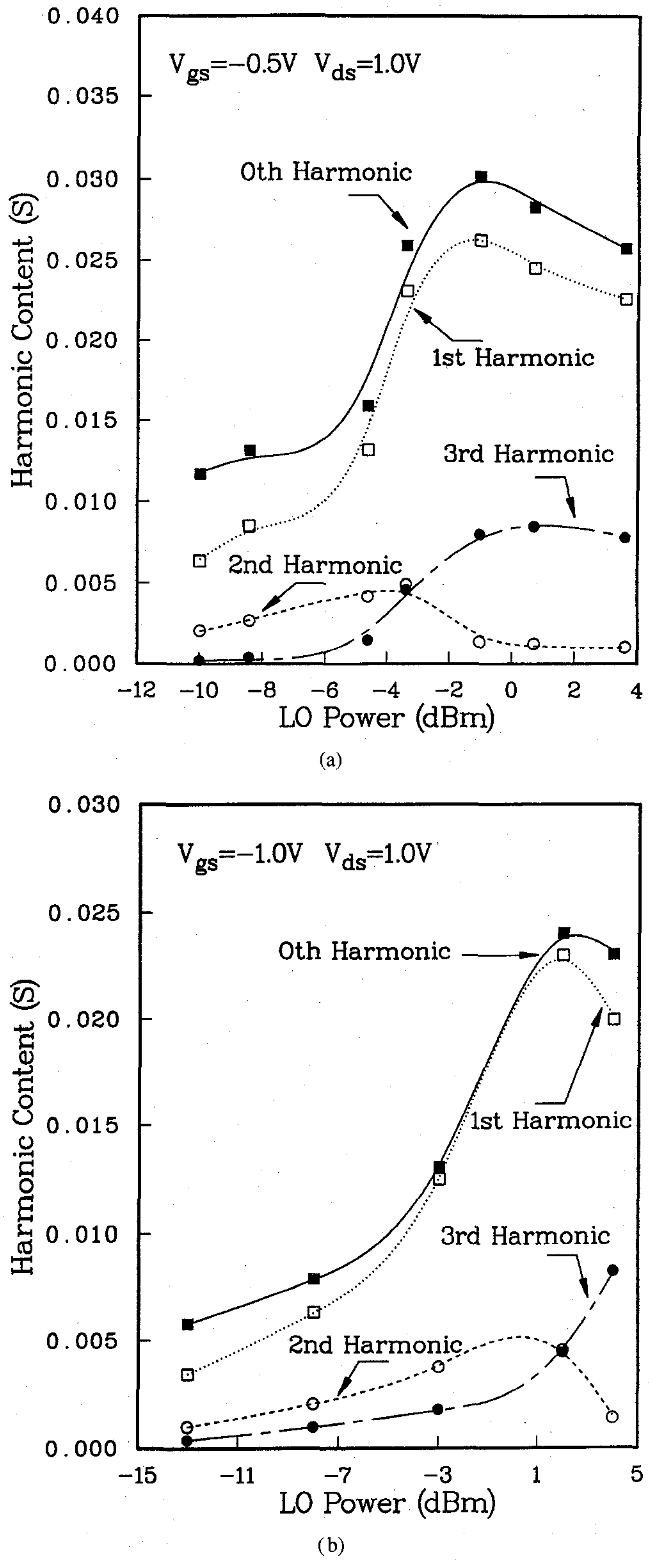

Fig. 3. Harmonic components of transconductance as a function of LO power. (a) HEMT A. (b) HEMT B.

The g_{m_1} cut-off frequency ($f_{T,g_{m_1}}$) can in this way be used as a figure of merit for the conversion gain and high frequency operation limits of the mixer. HEMT A has a $f_{T,g_{m_1}}$ of 110 GHz and HEMT B of 95 GHz and thus a slightly higher conversion gain is expected from the former at 94 GHz.

As a final step of the theoretical analysis, a two-tone harmonic balance simulation which includes accurate models for passive elements, was performed to evaluate the conversion gain and its LO power dependence in monolithic mixers. A comparison of the simulation results with the experimental performance is presented in the next section.

IV. Experimental Performance of the Monolithic InAlAs/InGaAs HEMT Mixer

The HEMT design has been discussed previously [4]. It is based on a 400 Å thick InGaAs channel, followed by a 50 Å InAlAs spacer, a 150 Å (5×10^{18} cm^{-3}) InAlAs donor layer, and 250 Å of undoped InAlAs under the gate. Two different wafers were tested with device characteristics corresponding to the features of HEMT A and HEMT B described in the previous section. The Hall measurements showed that HEMT A had a slightly higher mobility (11 000 vs 9300 cm^2/V · sec) and sheet charge density (3.9×10^{12} versus 2.7×10^{12} cm^{-2}).

A monolithic circuit using an InAlAs/InGaAs HEMT for mixing was designed and fabricated with in-house developed submicron technology. The HEMT had two 45 μm wide gate fingers. Optical lithography was used for all the process steps except for the 0.1 μm mushroom gates; these were written by means of a JEOL JBX 5DIIF E-beam system. First, a 2300 Å mesa was formed using diluted Phosphoric acid etchant. Ohmic patterns were defined with a AZ 5214 photoresist image reversal process to ensure good edge definition and yield without critical dependence on chlorobenzene. Ge/Au/Ni/Ti/Au ohmic metals were then evaporated and followed by two-step rapid thermal annealing. Following this, 0.1 μm long mushroom-shaped gates were realized using a bi-layer E-beam process. Diluted citric etchant was used to remove the n$^+$ InGaAs cap layer and recess the gate. The gate recess was monitored and terminated when the desired current level and breakdown voltage were reached. Ti/Pt/Au was then used for gate metallization and also for the bottom plate metal of the overlay capacitors. The capacitors were realized with 2500 Å thick SiO_2 sputtered selectively over the desired areas. The interconnects and top capacitor plates were made using evaporated Ti/Au (0.1/1 μm). Airbridge technology was used for the final interconnection step. The wafers were finally thinned to 100 μm and diced to obtain the individual chips. At the end of the whole MMIC processes, the f_T values of HEMT A and B were 150 GHz and 125 GHz respectively and the estimated $f_{\max}$ values were of the order of 180 GHz for both cases. The gate recess was deeper for HEMT A and the pinch-off voltage (V_p) was −0.5 V for HEMT A and −1 V for HEMT B.

The photograph of a completed monolithic HEMT mixer chip is shown in Fig. 4. The chip size is 1.4 mm × 1.0 mm. The device is biased close to pinch-off so that g_{m_1} can be maximized. This also ensures a small gate-source capacitance and its time average ($\overline{c}_{gs}$). Operation is based on the modulation of the device g_m and I_{ds} by the LO signal and the generation of mixed RF and LO products at the drain terminal. The passive circuitry is designed to provide proper terminations at the gate and drain as necessary for

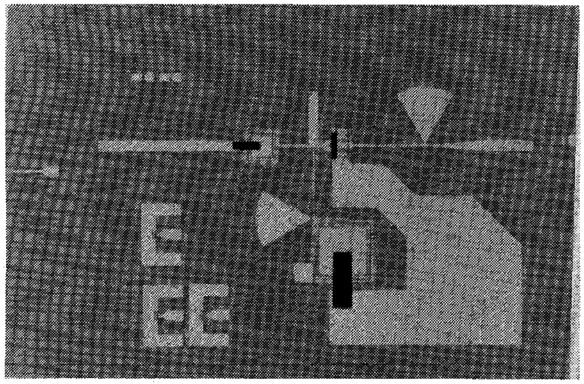

Fig. 4. Photograph of monolithic InP-based InAlAs/InGaAs HEMT mixer (1.4 mm × 1.0 mm).

maximum conversion gain. The short circuit is provided at the IF frequency using a large biasing capacitor at the gate. An IF frequency of 3 GHz was used in the design. The RF matching is achieved with microstrip stubs and the gate bias is decoupled on chip with radial stub biasing circuitry. The low-pass filter is realized with a simple resonating radial stub (center frequency = 91 GHz) at the drain. This might not be enough to reject all the harmonics of the LO and the RF, but is sufficient for demonstrating monolithic mixer operation at 94 GHz. This is particularly true for HEMT mixers where the optimum LO pumping power is not too large and the generation of higher harmonics of the LO is not dominant. Because of space and stability considerations, no IF matching circuit is integrated on chip. The use of a large load impedance for IF matching while satisfying the stability condition and its combination with a Hi-Z/Lo-Z low pass filter should in fact improve the conversion gain at the cost, of course, of area. The designed RF pass band of the mixer is from 86.5 GHz to 95.5 GHz with an LO frequency of 91 GHz (10% bandwidth).

The monolithic mixer chip is mounted in a specially designed test fixture which has a waveguide-to-finline-to-microstrip transition. Details of this transition are described by the authors elsewhere [13]. The insertion loss of the fixture is nominally 2 dB for the RF port over most of W-band. For testing, the RF and LO signals are coupled to the gate port through an external directional coupler. The drain bias is achieved with an external bias tee at the IF line. A spectrum analyzer is used to monitor the power and the frequency of the downconverted IF signal.

Measured conversion gain as a function of input frequency is illustrated in Fig. 5 for both devices. Fig. 5(a) shows the conversion gain dependence on the RF frequency with the LO frequency fixed at 91 GHz. The HEMT A mixer shows a nominal gain of -0.5 dB across the passband while the gain of the HEMT B circuit has a value which is by about 1 dB lower. The gain decrease at 93 and 89 GHz probably arises from resonances in the external IF transitions and connections at 2 GHz. With the exception of these two points, the gain is fairly flat (within ± 0.5 dB) over the pass band. The fast roll-off of the gain at frequencies greater than 95 GHz or less than 87 GHz is believed to be caused by the high loss of

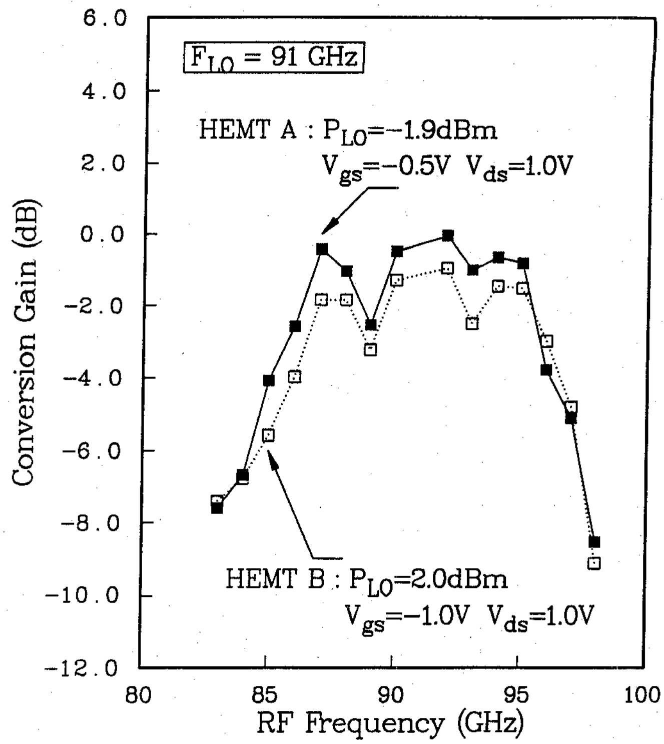

(a)

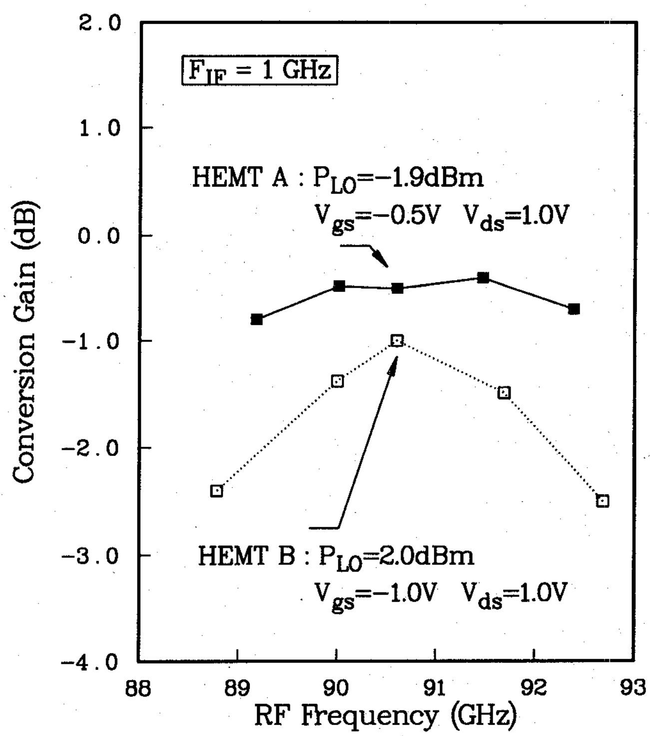

(b)

Fig. 5. Measured RF frequency dependence of conversion gain. (a) Fixed LO = 91 GHz. (b) Fixed IF = 1 GHz.

the IF transition, the external cables and the bias tee at high frequencies.

In order to investigate the conversion gain dependence on the RF frequency only and avoid the problems discussed above, the conversion gain is measured with the IF frequency

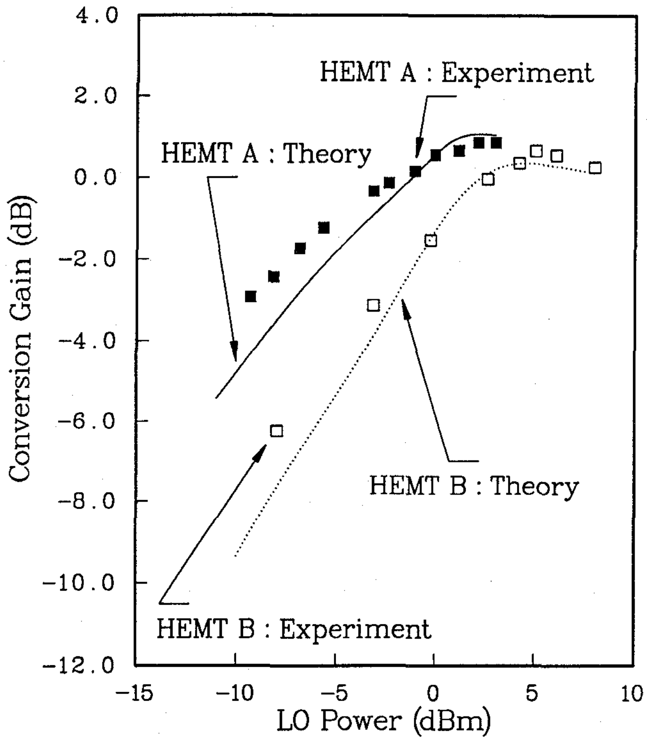

Fig. 6. LO power dependence of conversion gain (theory and experiment). RF and LO frequencies are 94 GHz and 91 GHz, respectively. The bias conditions are $V_{gs} = -0.5$ V and $V_{ds} = 1.0$ V for HEMT A and $V_{gs} = -1.0$ V and $V_{ds} = 1.0$ V for HEMT B.

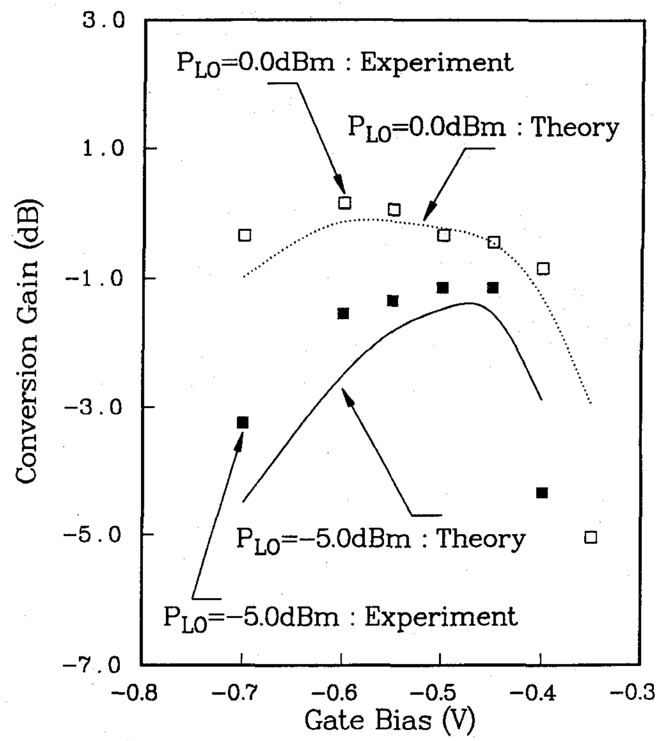

Fig. 7. Gate bias dependence of conversion gain (theory and experiment). V_{ds} is fixed at 1.0 V. RF and LO frequencies are 94 GHz and 91 GHz, respectively.

fixed at 1 GHz (Fig. 5(b)); in this case, the LO frequency exceeds the RF frequency by 1 GHz. Conversion gain for both devices shows smooth characteristics across the pass band (maximum ± 1 dB variation) with optimum performance achieved near 91 GHz which is the design center frequency (see Fig. 5(b)). These measurements confirm that the matching networks and the embedding impedances characteristics are close to the predicted ones.

Measured conversion gain as a function of LO power for both devices is plotted in Fig. 6. Also shown is the theoretical gain calculated from the two-tone harmonic balance analysis using the large-signal HEMT model discussed in the previous section. Conversion gain of the HEMT A mixer reaches the maximum value of 0.9 dB at 2 dBm of LO drive and that of HEMT B peaks up at 5 dBm with a maximum conversion gain value of 0.7 dB. The decrease of gain as LO power decreases is slower for HEMT A in the LO power range of -5 dBm to 5 dBm. This can be explained by the LO power dependence of g_{m_1}; as expected from Fig. 3, the g_{m_1} increases rapidly with the LO drive for HEMT A at LO power levels exceeding -4.5 dBm. (see Fig. 3(a)) From Fig. 3, the optimum LO drive for HEMT A should occur at -1 dBm. However, the experimental results indicate an optimum power level of 2 dBm. This 3 dB discrepancy can be accounted for by the LO mismatches and losses since the input port is designed for small signal (RF) impedance matching. Similar considerations can be made for HEMT B.

Following the results of Figs. 3 and 6, HEMT A is better in terms of nonlinearity and requires less LO power to achieve the same level of conversion gain. Both devices, however, show almost identical peak conversion gain. This conforms with g_{m_1} cut-off frequency ($f_{T,g_{m_1}}$) considerations outlined in Section III. Equations (3) and (4) predict the conversion gain to be 6.6 dB for HEMT A and 5.3 dB for B; the values used for this prediction are $R_{\text{in}} = 15\,\Omega, R_{ds} = 8\,\text{K}\Omega$ and $R_{\text{load}} = 50\,\Omega$. The conversion gain values from this simplified model are not far off from the experimental results. Further improvement of the conversion gain will require: (i) HEMT's with higher peak transconductance and more rapid variation of g_m with v_{gs} and (ii) reduced mismatch losses at the input.

The gate bias dependence of the conversion gain for HEMT A is illustrated finally in Fig. 7 together with the simulation results. As the LO power is increased, the optimum gate bias shifts slightly toward negative values (i.e., toward pinch-off). This can be explained from the efficiency of first harmonic generation by g_m. When the pumping power level is low, the bias should be selected to be slightly above the pinch-off. Otherwise, the value of g_m is too small to cause any mixing. At large pumping power levels, biasing should, however, be slightly negative with respect to the pinch-off voltage in order to generate higher order harmonics efficiently. The rapid degradation of conversion gain at biases greater than the pinch-off voltage is the result of entering the linear region of the g_m, thus reducing the harmonic generation efficiency.

In summary, the prediction of the magnitude and LO power dependence of conversion gain from the simplified model presented in Section III, is verified experimentally from the measurements. The bias dependence of g_m together with harmonic content studies gives an easy and fairly accurate first-order estimation of the HEMT mixer performance and can be utilized as a guide in the mixer design.

V. Conclusions

It has been shown that conversion gain is possible using InP-based InAlAs/InGaAs HEMT MMIC technology at 94 GHz. A simple large-signal analysis method based on harmonic content studies is developed and applied to HEMT mixers, providing physical insight to the mixing mechanisms and explaining the relationship between the conversion gain and device parameters. High frequency design criteria are established by defining the first harmonic transconductance cut-off frequency ($f_{T,g_{m_1}}$). HEMT's with different characteristics were used in the mixer realization and the experimental results are compared, yielding the design performance expected from device parameter considerations. Measured power and frequency characteristics of conversion gain also show the expected performance with the best conversion gain of 0.9 dB at the RF frequency of 94 GHz and with an LO drive of 2 dBm. The conversion gain variation is within ± 1 dB over the passband of the mixer.

Acknowledgment

The authors wish to thank Y. J. Chan, Dr. W. Q. Li and Prof. P. Bhattacharya for MBE growth and Prof. G. Rebeiz and his graduate students for providing test equipment parts.

References

[1] S. A. Maas, "Design and performance of a 45-GHz HEMT mixer," *IEEE Trans. Microwave Theory Tech.*, vol. MTT-34, no. 7, pp. 799–803, July 1986.
[2] P. D. Chow, D. Garske, J. Velebir, E. Hsieh, Y. C. Ngan, and H. C. Yen, "Design and performance of a 94 GHz HEMT mixer," in *1989 IEEE MTT-S Int. Microwave Symp. Dig.*, June 1989, pp. 731–734.
[3] P. Ho, M. Y. Kao, P. C. Chao, K. H. G. Duh, J. M. Ballingall, S. T. Allen, A. J. Tessmer, and P. M. Smith, "Extremely high gain 0.15 μm gate-length InAlAs/InGaAs/InP HEMT's," *IEE Electron. Lett.*, vol. 27, pp. 325–327, 1990.
[4] G. I. Ng, D. Pavlidis, M. Jaffe, J. Singh, and H. F. Chau, "Design and experimental characteristics of strained $In_{.52}Al_{0.48}As/In_xGa_{1-x}As$ ($x > 0.53$) HEMT's" *IEEE Trans. Electron Devices*, vol. ED-36, no. 10, pp. 2249–2259, Oct. 1989.
[5] M. Weiss, G. I. Ng, and D. Pavlidis, "New generation MMIC amplifiers using InGaAs/InAlAs HEMT's," *IEEE Electron. Lett.*, vol. 26, no. 4, pp. 264–266, 1990.
[6] K. H. G. Duh, P. C. Chao, P. Ho, A. Tessmer, S. M. J. Liu, M. Y. Kao, P. M. Smith, and J. M. Ballingall, "W-band InGaAs HEMT low noise amplifiers," in *1990 IEEE Int. Microwave Symp. Dig.*, May 1990, pp. 595–598.
[7] Y. Kwon, D. Pavlidis, M. Tutt, G. I. Ng, R. Lai, and T. Brock, "W-band monolithic oscillator using InAlAs/InGaAs HEMT's," *IEE Electron. Lett.*, vol. 26, pp. 1425–1426, 1990.
[8] Y. Kwon, D. Pavlidis, P. Marsh, M. Tutt, G. I. Ng, and T. Brock, "180 GHz InAlAs/InGaAs HEMT monolithic integrated frequency doubler," in *Tech. Dig. 1991 IEEE GaAs IC Symp.*, Oct. 1991, pp. 165–168.
[9] Y. Kwon, D. Pavlidis, M. Tutt, G. I. Ng, and T. Brock, "W-Band monolithic mixer using InAlAs/InGaAs HEMT's," in *Tech. Dig. 1990 IEEE GaAs IC Symp.*, Oct. 1990, pp. 181–184.
[10] P. D. Chow, K. Tan, D. Streit, D. Garske, P. Liu, and H. C. Yen, "Ultra low noise high gain W-band InP-based HEMT downconverter," in *1991 IEEE MTT-S Int. Microwave Symp. Dig.*, June 1991, pp. 1041–1044.
[11] M. Berroth and R. Bosch, "High-frequency equivalent circuit of GaAs FET's for large-signal applications," *IEEE Trans. Microwave Theory Tech.*, vol. 39, no. 2, pp. 224–229, Feb. 1991.
[12] R. A. Pucel, D. Massé, and R. Bera, "Performance of GaAs MESFET mixers at X band," *IEEE Trans. Microwave Theory Tech.*, vol. MTT-24, no. 6, pp. 351–360, June 1976.
[13] Y. Kwon, D. Pavlidis, P. Marsh, M. Tutt, G. I. Ng, and T. Brock, "90–180 GHz Heterostructure Monolithic Integrated Doubler," in *Tech. Dig. 2nd Int. Symp. on Space Terahertz Technology*, Feb. 1991, pp. 238–254.

Youngwoo Kwon (S'90) was born in Korea, in 1965. He received the B.S. degree in electronic engineering at the Seoul National University in 1988, and the M.S.E.E. degree from the University of Michigan, Ann Arbor, in 1990.

Currently, he is working toward the Ph.D. degree in electrical engineering at the University of Michigan. His research interests include the design and fabrication of submicron HEMT's, and large-signal modeling and realization of monolithic microwave and millimeter-wave integrated circuits.

Dimitris Pavlidis (S'73–M'76–SM'83) received the B.Sc. degree in physics from the University of Patras, Greece, in 1972, and the Ph.D. degree from the University of Newcastle-upon-Tyne, U.K., in 1976. He continued as Postdoctoral Fellow at Newcastle until 1978, engaged in work on microwave semiconductor devices and circuits.

In 1978, he joined the High Frequency Institute of the Technical University of Darmstadt, West Germany, working on III-V devices and establishing a new semiconductor technology facility. In 1980 he worked at the Central Electronic Engineering Research Institute, Pilani, India, as UNESCO consultant. During 1980–85, he was Engineer and Manager of the GaAs Monolithic Microwave Integrated Circuits (MMIC) Group of Thomson-CSF DHM/DAG, Corbeville, France. In this capacity, he was responsible for projects on monolithic power and broad-band amplifiers, tunable oscillators, optical preamplifiers, phase shifters attenuators, their technology and process evaluation, and the establishment of a component library for MMIC applications. He has been Professor of Electrical Engineering and Computer Science at the University of Michigan, Ann Arbor, since 1986. His current research interests cover the design and fabrication of HEMT's, HBT's, strained heterostructures III-V microwave and millimeter devices and monolithic heterostructure integrated circuits.

His publications are in microwave semiconductor devices and circuits and he holds six patents on MMIC applications. In 1990 Dr. Pavlidis was awarded the Microwave Prize for his work on InP Based Monolithic Integrated HEMT Amplifiers. In 1992 he was awarded the honor of "Palmes Académiques" in the order of Chevalier by the French Minister of National Education for distinguished work in the field of education.

Phil Marsh completed an industrial electronic technician's program in the Helena Vo Tech Center, Helena, MT, in 1978. In 1982 and 1985 he received the B.Sc.(Hon.) and M.S.E.E. degrees in electrical engineering from Montana State University.

From 1983 to 1987 he was involved in circuit design of custom military radio hardware and various other low-volume Rf projects at Tele Tech Corp. in Bozeman, MT. In 1988 he joined Texas Instruments' Defense Systems and Electronics Group. Here his work involved testing of X-band radar modules and various related microwave projects. Currently, he is working toward the Ph.D. E.E. degree at the University of Michigan. His research interests include device noise mechanisms, HBT and HEMT design and the integration of microwave functions.

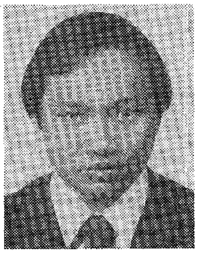

Geok-Ing Ng was born in Singapore. He received the B.S., M.S. and Ph.D. degrees in electrical engineering in 1984, 1986 and 1990, respectively, from the University of Michigan, Ann Arbor.

Since 1985 he has been working as a Research Assistant at the Center for High Frequency Microelectronics, Solid-State Electronics Laboratory, Department of Electrical Engineering and Computer Science, University of Michigan. His research interests include device physics, fabrication and characterization of microwave devices with different III-V material systems for low-noise, power and monolithic microwave integrated circuit applications. He is presently working as a Research Fellow at the Center for Space Terahertz Technology, University of Michigan and is a member of Tau Beta Pi and Eta Kappa Nu.

Dr. Ng was awarded the 1990 European Microwave Prize for his work on InP based heterostructure monolithic amplifiers.

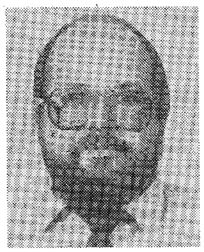

Timothy L. Brock has been a Research Engineer at the University of Michigan since Oct. 1989. His primary responsibilities involve electron beam lithography relating to submicron circuit and device fabrication. Prior to this he held a research position at the University of Illinois and has been involved with several publications involving electron beam applications.